may be sufficient to produce, among a whole distribution of structures, two favored solute–solvent cage configurations which can account for the observed differences in lifetime and spectral shape.

Acknowledgment. The authors wish to express their thanks to Professor K. Weiss for many helpful suggestions and stimulating discussions throughout this work.

Ultrasonic Absorption in Aqueous Polyelectrolyte Solutions. I

Gordon Atkinson,* Erwin Baumgartner, and Roberto Fernandez-Prini

Contribution from the Department of Chemistry, University of Maryland, College, Park, Maryland 20742. *Received March 29, 1971*

Abstract: Ultrasonic absorption has been measured in aqueous solutions of salts of polyacrylic acid (HPA) and carboxymethylcellulose (CMC) in the frequency range 1–190 MHz at 25°. The effects of molecular weight, degree of neutralization, concentration, and nature of the cation were studied. The polyelectrolyte solutes produce excess absorption characterized by very wide absorption bands, which greatly hampers a quantitative analysis of the dynamic processes being observed. These processes are shown to be due to counterion interaction with the repetitive segments of the polyion chain rather than to processes due to the chain as a whole. Alkaline earth counterions produce large increases in absorption. This absorption is qualitatively different from that found due to isolated interaction between single $RCOO^-$ groups and the same counterions. Several mechanisms for the polyelectrolyte absorption are suggested and discussed.

The activity coefficients and the mobilities of counterions in polyelectrolyte solutions are much lower than those found at equivalent concentrations of simple electrolytes. These facts are normally explained in terms of counterion binding to the polyion due to the large electric field on the polyion chain. The extent of counterion binding can be explained satisfactorily[1] by models which use a uniformly charged cylinder or sheet as a model for the polyion. The solution is divided into electrically neutral domains and the electrostatic equations are solved for one domain.[1,2] In general, it is observed that the equilibrium and transport properties of polyelectrolytes are predicted semiquantitatively by those models. That is, counterion binding is essentially determined by the overall charge density on the chain. As the concentration of polyelectrolyte increases, the major change predicted by such models is the decrease in extension of the domains so that the counterions are, on the average, closer to the polyion.

In polysulfonate solutions, the counterion binding of the alkali metal ions increases with increasing crystallographic radius of the metal ion,[3,4] suggesting that the counterions are not desolvated when binding to the polyion. Ir and nmr evidence in strong sulfonic acid ion exchange resins supports this view.[5] In solutions of polycarboxylates[6,7] and polyphosphates[8] the trend of increased counterion binding is reversed so that the smallest ions show the highest association. This implies that in addition to overall atmosphere binding, some site binding involving partial desolvation of counterions occurs. Thus the multistep mechanism proposed by Eigen[9] to explain ion association in simple electrolytes can be adapted for counterion binding in polyelectrolytes as depicted in Figure 1. The species B in Figure 1 involves a continuous distribution of counterions interacting with the overall charge density on the polyion. This is the dominant species in polysulfonates. Species C represents some direct contact between conterions and ionogenic groups on the chain and apparently contributes to the counterion binding in polycarboxylate and polyphosphate solutions.

Counterion binding reduces the electrostatic repulsion between neighboring charged sites on the chain. This shielding, which becomes more effective with increased binding, leads to a decrease in the average dimensions of the polymer chain. The change in average extension of the chains is easily seen in the reduced viscosity of the solutions.[3,10] The expansion of the polyion chain is particularly notable when the degree of neutralization of weak polyacids increases.[11] Hence, counterion binding is a complex process which involves the multistep approach of counterions coupled with changes in the average dimensions of the polyion.

Relaxation methods are particularly suitable for studying the dynamics of the complex process of counterion binding. If the various steps in the process are separable on a time scale, the relaxation methods could allow the study of their individual contributions to the overall process. The magnitude of the volume change accompanying the binding of each counterion[4] is large enough[12] to produce a measurable increase in the

(1) R. Fernández-Prini, E. Baumgartner, S. Liberman, and A. E. Lagos, *J. Phys. Chem.*, 73, 1420 (1969).
(2) G. Manning, *J. Chem. Phys.*, 51, 924, 934, 3249 (1969).
(3) R. Fernández-Prini and A. E. Lagos, *J. Polym. Sci., Part A*, 2, 2917 (1964).
(4) U. P. Strauss and Y. P. Lueng, *J. Amer. Chem. Soc.*, 87, 1476 (1965).
(5) G. Zundel and A. Murr, *Electrochim. Acta*, 12, 1147 (1967).
(6) L. A. Noll and S. J. Gill, *J. Phys. Chem.*, 67, 498 (1963).
(7) H. P. Gregor, D. H. Gold, and M. Frederick, *J. Polym. Sci.*, 23, 467 (1957).
(8) U. P. Strauss and P. D. Ross, *J. Amer. Chem. Soc.*, 81, 5295, 5299 (1959).
(9) M. Eigen, *Discuss. Faraday Soc.*, No. 24, 25 (1957).
(10) C. Tanford, "Physical Chemistry of Macromolecules," Wiley, New York, N. Y., 1961, 489 ff.
(11) I. Noda, T. Tsuge, and M. Nagasawa, *J. Phys. Chem.*, 74, 710 (1970).

coefficient of ultrasonic absorption. We have measured the ultrasonic absorption coefficients in solutions of polyacrylates (PA) and carboxymethylcellulose (CMC) in the range from 10 to 190 MHz with some measurements being made to 1 MHz. PA and CMC were chosen because of the importance of the carboxylate group in biopolymers, because site binding can be be expected to take place to some extent with these polyions, and because the electrostatic shielding due to counterion binding is known to affect the dimensions of CMC much less than those of PA.[13]

Typical polyelectrolyte solutions have not been studied by ultrasonic absorption. Michels and Zana[14] have employed the technique to study neutral poly(acrylic acid) and poly(methacrylic acid). Ultrasonic absorption has been measured in synthetic poly(amino acid) solutions[15-18] in an effort to study the dynamics of the helix–coil transition. In some of these studies the ultrasonic absorption was found to vary with frequency in a way consistent with one or two relaxations due to chemical processes.[14,16,18] In other cases a distribution of relaxation times was found to more adequately represent the data[17] and agree with the theoretical predictions for a conformational change.[19] Since in the poly(amino acid) systems carboxylate and other charged groups interact with counterions, the ultrasonic absorption due to conformational change could be completely obscured by counterion–polyion interaction. This seems almost to be expected, as the volume change due to the conformational change is much smaller than that for the latter process[20] and so would lead to a smaller absorption amplitude.

Experimental Procedures

The polyelectrolytes were obtained through the courtesy of Rohm and Haas (PA) and the Hercules Powder Co. (CMC). Samples of HPA of degree of substitution 1.0 and molecular weights 25,000, 130,000, and 250,000[21] were available. The Na–CMC (Type 7-M) had a molecular weight of 100,000 and a degree of substitution of 0.7, according to the manufacturer's specifications. The HPA solutions of different degrees of neutralization were prepared by weight from a stock HPA solution and standardized NaOH solution. The alkaline earth salts of CMC were originally prepared by extensive dialysis of Na–CMC with excess alkaline earth nitrate solution against distilled water. Since these solutions did not differ in ultrasonic absorption from the same solutions before dialysis, later solutions were not dialyzed. There was also no difference between the ultrasonic absorption of pure alkaline earth PA solutions and those made from Na–PA solutions plus the correct amount of alkaline earth nitrates. This was the only way in which alkaline earth polyacrylate solutions could be prepared and studied without flocculation occurring.[22] Owing to flocculation, it was not possible to make measurements in solutions containing HPA and alkaline earth nitrates if the degree of neutralization of the acid was larger than 0.2–0.3.

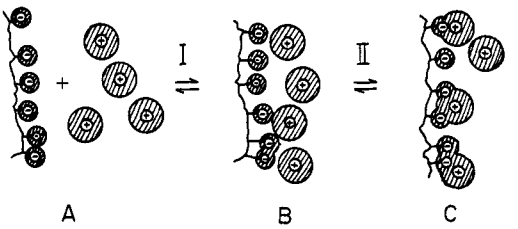

Figure 1. Multistep mechanism for counterion binding in polyelectrolyte solutions.

The ultrasonic absorption of the solutions was measured in the range 1–190 MHz using pulse techniques. A standard send–receive pulse apparatus[23] was used for the range 10–190 MHz. For the 1–20-MHz region a differential cell[24] using distilled water as a reference allowed the simultaneous measurement of ultrasonic absorption and velocity. The sound velocity of the solutions never differed from that of H_2O by more than 1%. The accuracy of the absorption coefficient, α, was on the order of 2% for all solutions. Owing to the large solution volume needed for the differential cell, the number of solutions studied in the 1–20-MHz range was limited. Since CMC solutions are very viscous (in particular, Na–CMC), solutions of concentration higher than 3% were not studied except for one 8% Na–CMC solution which was almost a gel

In the frequency region where the apparatus overlapped (10–20 MHz), the absorption coefficients agreed to within experimental error except at 10 MHz. At this frequency the high-frequency apparatus always gave slightly higher results probably due to the dispersion error. The frequency of measurement was determined using a heterodyne beat method with a Gertsch FM-3 frequency meter. Both cells were thermostated to 25 ± 0.1° with circulating H_2O.

Analysis of Data

The ultrasonic absorption data for solutions of polymeric solutes have been analyzed in very different ways. The data in the literature have been fitted, typically, either to one or two single relaxations, or to a distribution of relaxation times. Unfortunately, the frequency range in which ultrasonic absorption is most commonly measured (10–150 MHz) permits the unequivocal characterization of even a single relaxation only under favorable conditions. Obviously, then, the frequency range must be much wider if more than a single relaxation or a distribution of relaxations is to be adequately characterized. We shall analyze the frequency dependence of absorption only for those solutions in which our data extend to 1 MHz.

When the observed relaxation phenomena are due to single chemical processes (Debye relaxations), the ultrasonic absorption coefficient is represented by

$$(\alpha/f^2) = \sum_{j=1}^{m} \frac{A_j}{1 + (f/f_{r,j})^2} + B \qquad (1)$$

where α = absorption coefficient (defined by the equation $I_x = I_0 e^{-2\alpha x}$ in terms of intensities and distance), f = measured frequency, B = background absorption due to processes above the frequency range being examined, A_j = amplitude factor of the jth relaxation, and $f_{r,j}$ = relaxation frequency of the jth relaxation. The amplitudes depend only on the normal-coordinate thermodynamic parameters of the jth process and the relaxation frequencies depend also on its kinetics.

Michels and Zana[14] found that (α/f^2) for HPA and poly(methacrylic acid) (HPMA) solutions could be fitted

(12) For polyacrylates the overall change in volume per bound ion is greater than 6 and 25 cm³/mol for alkali metals and alkaline earths, respectively.

(13) S. A. Rice and M. Nagasawa, "Polyelectrolyte Solutions," Academic Press, New York, N. Y., 1961, pp 330 ff.
(14) B. Michels and R. Zana, *Kolloid-Z. Z. Polym.*, **234**, 1008 (1969).
(15) T. K. Saksena, B. Michels and R. Zana, *J. Chim. Phys. Physico-chim. Biol.*, **65**, 597 (1968).
(16) G. G. Hammes and P. B. Roberts, *J. Amer. Chem. Soc.*, **91**, 1812 (1969).
(17) J. J. Burke, G. G. Hammes, and T. B. Lewis, *J. Chem. Phys.*, 42, 3520 (1965).
(18) R. C. Parker, K. Applegate, and L. J. Slutsky, *J. Phys. Chem.*, **70**, 3018 (1966).
(19) G. Schwarz, *J. Mol. Biol.* **11**, 64 (1965).
(20) H. Noguchi and J. T. Yang, *Biopolymers*, **1**, 359 (1963).
(21) R. Zana and E. Yeager, *J. Phys. Chem.*, **71**, 3502 (1967).
(22) F. T. Wall and J. N. Drenan, *J. Polym. Sci.*, 7, 83 (1951).
(23) R. Garnsey and D. W. Ebdon, *J. Amer. Chem. Soc.*, **91**, 50 (1969).
(24) R. Corsaro, G. Atkinson, and B. R. Perlis, *Chem. Instrum.*, **2**, 389 (1970).

Table I. Typical Discrete Relaxation Fit; 0.5 *N* Aqueous Na–PA

Frequency range, *m*, MHz		$A \times 10^{17}$ [a]	f_{r_2}, MHz	$A_1 \times 10^{17}$ [a]	f_{r_1}, MHz	$B \times 10^{17}$ [a]	$\sigma \times 10^{17}$ [a]
1–170	2	562 ± 161	1.12 ± 0.33	117 ± 15	21.8 ± 3.5	(39)[b]	8.0
2–170	2	198 ± 22	4.3 ± 0.8	66 ± 13	40.0 ± 8.3	(39)[b]	5.5
10–170	1			112.5 ± 5.9	20.1 ± 1.7	45.6 ± 2.0	3.7

[a] Nepers sec^2 cm^{-1}. [b] Fixed arbitrarily.

to two discrete relaxations (*i.e.*, $m = 2$ in eq 1) with relaxation frequencies in the 1–2- and 10–25-MHz ranges. We have fitted our results using computer least-squares methods to eq 1 using $m = 1$ and $m = 2$. Figure 2 illustrates the results of the analysis for 0.5 *N* Na–PA (0.5 mol of monomer/l.). In Table I the values of the parameters and the standard deviation of the fit are reported.

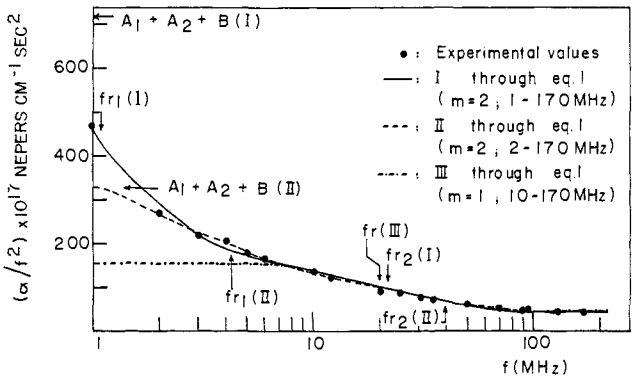

Figure 2. Typical discrete relaxation fit for 0.5 *N* aqueous Na–PA solutions.

If only one of the frequency ranges is considered, either in Figure 2 or Table I, the fit appears satisfactory. However, the extreme sensitivity of the determined parameters on the experimental frequency range renders the procedure rather meaningless. The same results were obtained in our analysis of all the other solutions examined in the present work.

Besides the unsatisfactory nature of the data-fitting process using eq 1, the equation appears unacceptable from more general considerations. Any dynamic process taking place in solutions of polymeric solutes and involving the solute should have a distribution of relaxation times, even assuming the unlikely case of infinitely narrow molecular weight distribution. This is expected because of the different environments in which the various repeating segments of the polymeric solute find themselves. Only dynamic processes involving individual segments (*e.g.*, counterion binding, solvent–charge interaction) in highly ordered structures (perfect helix) could be expected to have a distribution of relaxation times sharp enough to correspond more closely to a single Debye relaxation.

Dielectric relaxation studies have shown many instances of liquids and solutions having distributions of relaxation times. Cole and coworkers[25,26] have obtained the corresponding distribution functions for the relaxation times. The corresponding distribution functions for the ultrasonic measurements have not been as well established experimentally to date. This is because of the experimental difficulties associated with making absorption and velocity measurements over a very wide frequency range. It is, however, common practice to employ the distribution functions found from dielectric work in the interpretation of ultrasonic data.[27] The symmetric Cole–Cole distribution (SCC)[25] has been successfully employed in explaining dielectric relaxation in polyelectrolyte solutions.[28] Burke, Hammes, and Lewis[17] used the asymmetric Davidson–Cole (ADC) distribution to analyze ultrasonic absorption in aqueous poly(*l*-glutamic acid) solutions. However, as will be shown below, they did not employ the correct equation.

The frequency-dependent transfer function, σ, which characterizes the dynamic response of a solution property (*e.g.*, permittivity, compressibility, viscosity) to an external time-dependent perturbation is

$$\sigma = (\sigma_{real} - j\sigma_{imag}) \quad (2)$$

For both Cole-type distribution of relaxation times

$$\sigma = 1/[1 + (j\omega\tau_r)^n] \text{ (SCC)} \quad (3)$$

$$\sigma = 1/[(1 + j\omega\tau_r)^\beta] \text{ (ADC)} \quad (4)$$

where τ_r = a characteristic relaxation time.

The exponents n and β are such that $0 \leq n, \beta \leq 1$ and give the width of the distribution. When n or β is unity, eq 3 and 4 describe single Debye relaxations. Figure 3 depicts the distribution functions $F(\tau/\tau_r)$ for processes having a relaxation time between τ and $\tau + d\tau$ corresponding to the ADC and SCC distributions for n and β equal to 0.70. The SCC distribution is similar in shape to a gaussian distribution.[25] The ADC distribution function, on the other hand, is continuous for $\tau \leq \tau_1$ but zero outside this region. Hence, the ADC distribution relaxation spectrum is almost that of a Debye single relaxation for $\omega < 1/\tau_r$.

From eq 3 and 4 it is found that

$$\sigma_{real} = \frac{[1 + (\tan\varphi)^n \cos(n\pi/2)]}{[1 + 2(\tan\varphi)^n \cos(n\pi/2) + (\tan\varphi)^{2n}]} \text{ (SCC)} \quad (5)$$

$$\sigma_{real} = (\cos\varphi)^\beta \cos(\beta\varphi) \quad \text{(ADC)} \quad (6)$$

$$\sigma_{imag} = \frac{[(\tan\varphi)^n \sin(n\pi/2)]}{[1 + 2(\tan\varphi)^n \cos(n\pi/2) + (\tan\varphi)^{2n}]} \text{ (SCC)} \quad (7)$$

$$\sigma_{imag} = (\cos\varphi)^\beta \sin(\beta\varphi) \quad \text{(ADC)} \quad (8)$$

$$\text{with } \tan\varphi = \omega\tau_r = (f/f_r)$$

When σ is the complex transfer function for compressi-

(25) K. S. Cole and R. H. Cole, *J. Chem. Phys.*, 9, 341 (1941).
(26) D. W. Davidson and R. H. Cole, *ibid.*, 19, 1484 (1951).
(27) T. A. Litovitz and C. M. Davis in "Physical Acoustics," Vol. IIA, W. P. Mason, Ed., Academic Press, New York, N. Y., 1965, Chapter 5.
(28) S. B. Sachs, A. Raziel, H. Eisenberg, and A. Katchalsky, *Trans. Faraday Soc.*, 65, 77 (1969).

bility, σ_{imag} is proportional to the ultrasonic energy dissipated in the process per wavelength,[29] $(\alpha\lambda)_r$. The total attenuation includes the high-frequency absorption (background absorption) denoted by B. Hence from eq 7 and 8

$$(\alpha\lambda) = \frac{A' \sin (n\pi/2)(\tan \varphi)^n}{1 + 2(\tan \varphi)^n \cos (n\pi/2) + (\tan \varphi)^{2n}} + B'f \quad \text{(SCC)} \quad (9)$$

$$(\alpha\lambda) = A'(\cos \varphi)^\beta \sin (\beta\varphi) + B'f \quad \text{(ADC)} \quad (10)$$

It is also common to express the absorption in terms of the quantity (α/f^2) which does not require the determination of sound velocity. For this quantity

$$\alpha/f^2 = \frac{A \sin (n\pi/2)(\tan \varphi)^{n-1}}{1 + 2(\tan \varphi)^n \cos (n\pi/2) + (\tan \varphi)^{2n}} + B \quad \text{(SCC)} \quad (11)$$

$$\alpha/f^2 = \frac{A(\cos \varphi)^\beta \sin (\beta\varphi)}{\tan \varphi} + B \quad \text{(ADC)} \quad (12)$$

where A is an amplitude factor (*cf.* eq 1) dependent only on the equilibrium properties that characterize the process.

If the relaxational part of the ultrasonic absorption is calculated by substracting the background, the functions $\log (\alpha\lambda)_r$ and $\log (\alpha/f^2)_r$ are universal functions of $\log f$. Table II gives the most important characteristics of the

Table II. Characteristics of ADC and SCC Distributions for Ultrasonic Absorption

	$\left[\frac{d \ln (\alpha\lambda)_r}{d \ln f}\right]$		$\left[\frac{d \ln (\alpha/f^2)_r}{d \ln f}\right]$	
	f/f_a		f/f_r	
Distribution	$\to\infty$	$\to 0$	$\to\infty$	$\to 0$
SCC	$-n$	$+n$	$-(n+1)$	$(n-1)$
ADC	$-\beta$	$+1$	$-(\beta+1)$	0
Debye (n or $\beta = 1$)	-1	$+1$	-2	0

log–log plots. In Figure 3, $(\alpha\lambda)_r$ for ADC and SCC distributions for n and β = 1.0, 0.80, and 0.40 are shown. Equations 5–12 show that $(\alpha/f^2)_r$ is proportional to σ_{real} only for a Debye single relaxation. Burke, Hammes, and Lewis[17] employed the σ_{real} part of the ADC distribution to analyze the ultrasonic absorption of aqueous poly(*l*-glutamic acid) solutions. If σ_{real} is used, the slope of $\log (\alpha/f^2)_r$ *vs.* $\log f$ should be $-\beta$ for $(f/f_r) \to \infty$. The fact that the data for poly(*l*-glutamic acid) could be fitted using σ_{real} (ADC) almost proves that this distribution does *not* represent the data adequately. If the correct σ_{imag} were employed

$$[d \ln (\alpha/f^2)_r / d \ln f]_{(f/f_r \to \infty)} = -(1 + \beta)$$

and must always be more negative than -1.

Only the solutions for which measurements were performed down to 1–2 MHz have been analyzed with a distribution of relaxation times. None of the results could be represented with ADC distribution. Table III summarizes the values found by least squares for the parameters in eq 11 for a single SCC.

(29) M. Eigen and L. de Maeyer, *Tech. Org. Chem.*, **8**, 954 (1963).

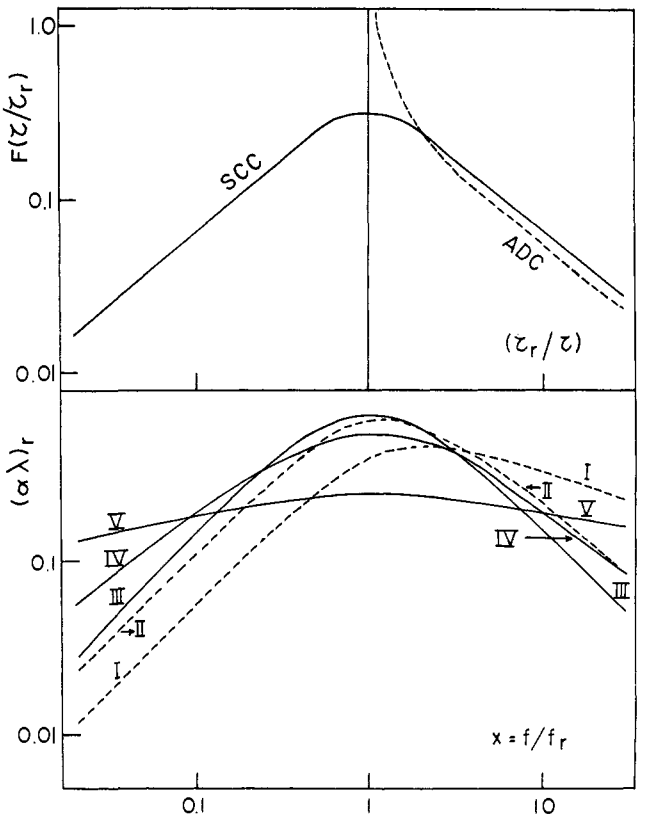

Figure 3. Upper part, SCC and ADC distribution functions $F(\tau/\tau)_r$. Lower part, $(\alpha\lambda)_r$ for SCC and ADC distributions for n and β = 1.0, 0.80, and 0.40: (I) β = 0.4, (II) β = 0.8, (III) n = β = 1.0, (IV) n = 0.8, (V) n = 0.4.

For i = 0.2 when Na^+ and Mg^{2+} are the counterions, the data for the PA solutions are well represented by the SCC distribution over the whole frequency range. For Na–Pa (i = 1.0) the fitting is less satisfactory and strongly dependent on the value assumed for B. For the Ca^{2+} counterion (i = 0.2) it was impossible to fit the experimental results to the SCC distribution. In these solutions α/f^2 is roughly proportional to f^{-1}. This would imply $n \simeq 0$ in eq 11, a nonacceptable value.

Effect of Concentration and Molecular Weight. The ultrasonic absorption of the 0.5 monomolar Na–PA solutions was the same for the three different molecular weight solutes (25,000, 130,000, 250,000) at any frequency in the 10–190-MHz range. Michels and Zana[14] had previously observed that the ultrasonic absorption of HPA and HPMA solutions was independent of molecular weight down to 1 MHz. Dielectric dispersion studies in polyelectrolyte solutions have given similar results. The conclusion is that the dynamic processes occurring at frequencies higher than 1 MHz do not involve the polymer chains as a whole but rather the repetitive segments of the chains.

An increase in polyelectrolyte concentration was observed to give an increase in (α/f^2). It is important to evaluate the concentration dependence of $(\alpha/f^2)_r$, but this requires that the background absorption B be subtracted from the observed (α/f^2). It may be considered that

$$B = B_{H_2O} + \Delta B \quad (13)$$

where B_{H_2O} = 23.0 × 10^{-17} neper sec^2 cm^{-1} is the low-

Table III. SCC Distribution Parameters for Polyacrylate Solutions[a-c]

i	Counterion	[Counterion], equiv l.$^{-1}$	$A \times 10^{17}$ [d]	$B \times 10^{17}$ [d]	f_r, MHz	n	$\sigma \times 10^{17}$ [d]
0.2	Na^+	0.1	125.1 ± 17.4	(26)	35.1 ± 8.6	0.67 ± 0.02	6.7
0.2	Na^+	0.1	102.8 ± 11.3	(26)	67.4 ± 11.2	(0.47)	6.8
	Mg^{2+}	0.1					
0.2	Na^+	0.1	139.7 ± 32.5	(21)	44.7 ± 15.6	0.52 ± 0.03	6.2
	Mg^{2+}	0.1					
1.0	Na^+	0.5	102.2 ± 19.4	(35)	55.0 ± 18.0	(0.57)	16

[a] Parameters are as defined in eq 11. [b] Polyelectrolyte concentration was 0.5 mol of monomer/l. [c] Values in parentheses were arbitrarily fixed to get a minimum in σ. [d] Nepers sec^2 cm^{-1}.

frequency absorption in H_2O at 25° and ΔB denotes any changes in the structural and shear relaxation of H_2O due to the presence of the solute and contributions from other relaxations above the measured frequency range. Figure 4 shows the effect of concentration on

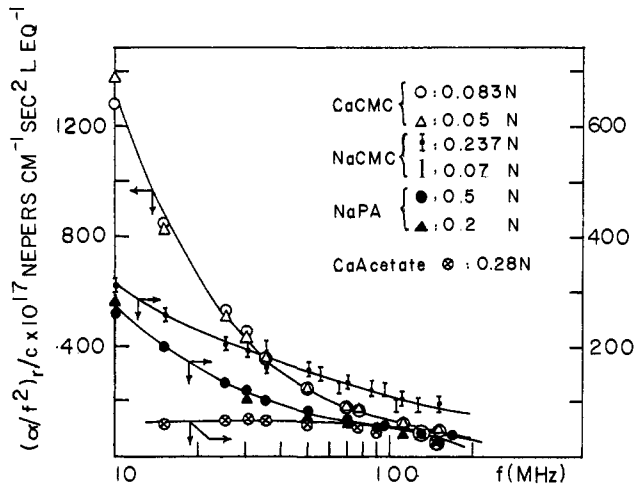

Figure 4. Effect of concentration on $(\alpha/f^2)_r/C$ for Ca-CMC, Na-CMC, Na-PA, and Ca-acetate solutions ($B = B_{H_2O^0} = 23 \times 10^{-17}$ neper sec^2 cm^{-1}).

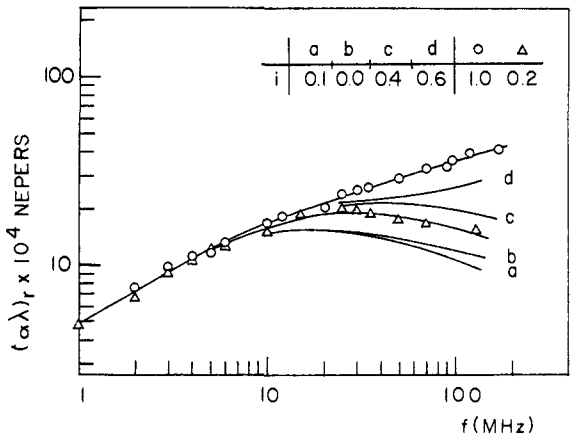

Figure 5. Log $(\alpha\lambda)_r$ *vs.* log f for 0.5 N HPA with different degrees of neutralization ($B = 26 \times 10^{-17}$ neper sec^2 cm^{-1}).

$(\alpha/f^2)_r/C$ for Na-PA, Ca-acetate, Ca-CMC, and Na-CMC at 25° assuming $B = B_{H_2O}$. Owing to the small absorption of solutions less than 0.10 monomolar in Na-CMC, the error in the excess absorption is larger than usual. The fact that $(\alpha/f^2)_r/C$ is found to be independent of concentration implies that ΔB is either negligible or linearly dependent on C. The time scale and amplitude of the processes occurring in the solutions show no experimentally detectable changes when the concentration of polyelectrolyte is varied.

This conclusion and the molecular weight independence of (α/f^2) strongly suggest that the model of polyionic domains could be employed to describe the dynamic processes occurring over the concentration and frequency ranges of this study.

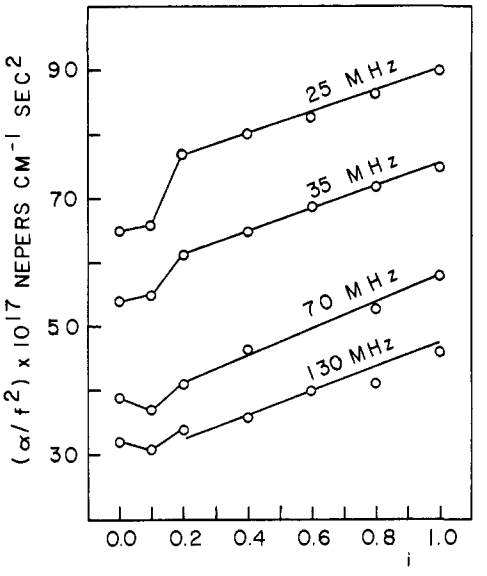

Figure 6. Ultrasonic absorption (α/f^2) *vs.* degree of neutralization for 0.5 N HPA at different frequencies.

Effect of Degree of Neutralization. Figure 5 is a plot of log $(\alpha\lambda)_r$ *vs.* log f for 0.50 monomolar HPA with different degrees of neutralization i. For the $i = 0.20$ and $i = 1.0$ solutions, the measurements were extended down to 1 MHz. The $i = 0.10$ solution has an excess absorption which is equal to or somewhat less than that of the pure acid. $(\alpha\lambda)_r$ for the pure acid shows a shallow maximum near 20 MHz which shifts to higher frequencies with increasing i until it disappears from the experimental frequency range at $i \geq 0.6$. At low frequencies $(\alpha\lambda)_r$ depends only slightly on i. However, at the higher frequencies it increases sharply with increasing i.

Figure 6 shows that for $i \geq 0.2$, α/f^2 varies linearly with i with a slope of 17×10^{-17} neper sec^2 cm^{-1} for all frequencies. In general

$$\alpha/f^2 = Ag(f) + B \qquad (14)$$

where $g(f)$ is the only frequency-dependent factor, and

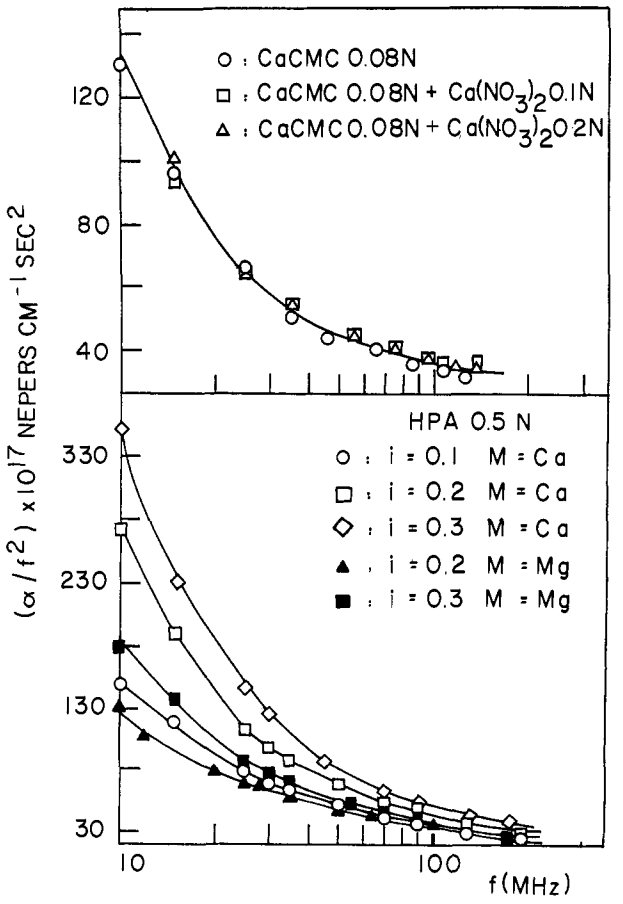

Figure 7. Upper part, effect of the addition of $Ca(NO_3)_2$ on the ultrasonic absorption of a 0.08 *N* Ca–CMC solution. Lower part, ultrasonic absorption in 0.5 *N* HPA at different degrees of neutralization and the effect of addition of alkaline earths as counterions.

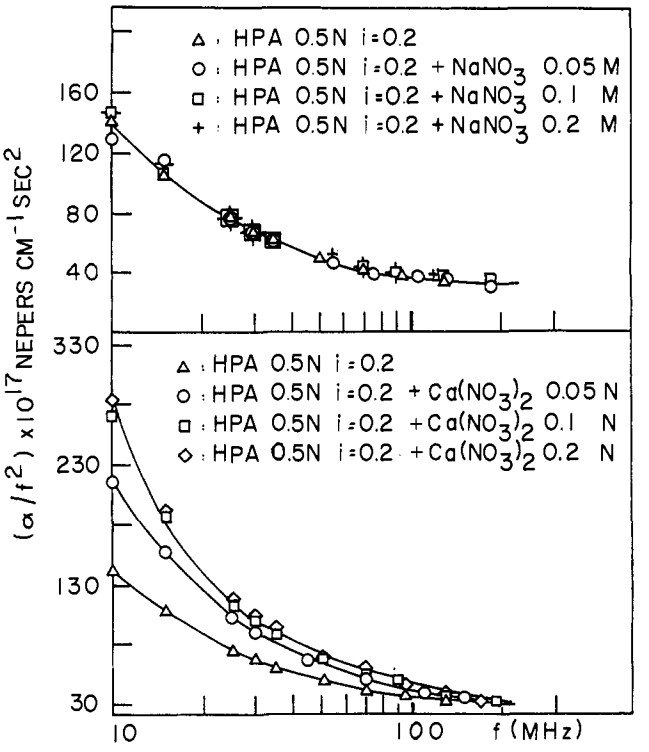

Figure 8. Upper part, effect of the addition of $NaNO_3$ on the ultrasonic absorption of a 0.5 *N* HPA solution (i = 0.2). Lower part, effect of the addition of $Ca(NO_3)_2$ on the ultrasonic absorption of a 0.5 *N* HPA solution (i = 0.2).

the variation of α/f^2 with i was found to be expressible by

$$\alpha/f^2 = Ag(f) + B_{H_2O} + \Delta Bi \qquad (15)$$

Hence the high-frequency shift in Figure 5 is due to the background absorption change being proportional to i, while the amplitude factor A is independent of i.

Effect of Counterions and Excess Salt. The presence of Ca^{2+} and Mg^{2+} in the solutions produces a sharp increase in the absorption much larger for Ca^{2+} than for Mg^{2+} at the same concentration. Figure 7 shows the variation of (α/f^2) with f for 0.5 monomolar HPA solutions with $i \leq 0.3$ (NaOH neutralization) and $M(NO_3)_2$ added so that there are equivalent amounts of Na^+ and M^{2+}. Data on Ca–CMC (0.08 *M*) prepared by dialysis are also included. The increase in (α/f^2) upon the addition of an alkaline earth counterion is particularly marked at low frequencies. The increase of (α/f^2) with i for Ca^{2+} and, to a lesser extent, for Mg^{2+} is much greater than for Na^+ and, in contrast to Figure 6, more pronounced at the lower frequencies.

In addition, there is strong evidence that the effect of counterions is specific. In Figure 7 it may be seen that the absorption of Ca–CMC is not altered by the addition of almost three times as much Ca^{2+} as $Ca(NO_3)_2$. When M^{2+} is added to Na–CMC (α/f^2) increases until the M^{2+} added is equivalent to the charged sites on the polyion and then does not change. When 0.35 equiv of $NaNO_3$ is added to 0.064 monomolar Na–CMC, no changes in (α/f^2) occur. Figure 8 illustrates the effects of adding $Ca(NO_3)_2$ or $NaNO_3$ to 0.50 monomolar HPA (i = 0.2).

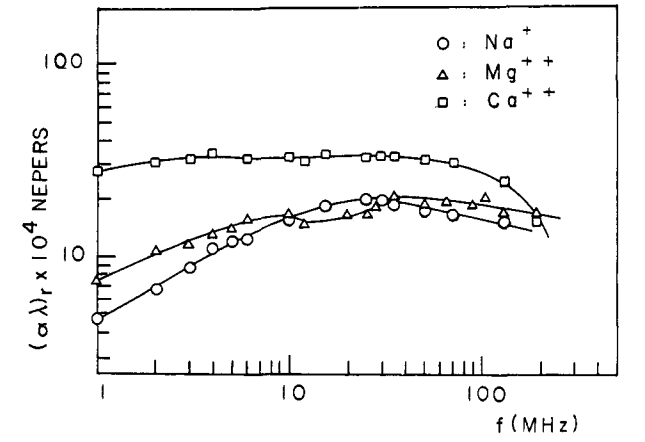

Figure 9. Log $(\alpha\lambda)_r$ *vs.* log f for 0.5 *N* HPA (i = 0.2) for different counterions ($B = 26 \times 10^{-17}$ neper sec² cm⁻¹).

Figure 9 shows the results over 1–190 MHz for 0.50 monomolar HPA neutralized to i = 0.2 with NaOH upon the addition of $Mg(NO_3)_2$ or $Ca(NO_3)_2$ in equivalent amounts. Although it is very difficult to quantitatively describe the processes taking place, it is clear that M^{2+} ions increase the absorption in the low-frequency range ($f \leq 10$ MHz). Furthermore, the data seem to show two wide bands of relaxation times on the addition of M^{2+} ions. This is clearly why it proved impossible to fit the data for the Ca^{2+} counterion effect using the single SCC distribution of eq 11.

Discussion

The results presented above demonstrate conclusively that the presence of the polyelectrolytes is responsible for all of the excess ultrasonic absorption found. We shall now discuss the possible sources of this excess absorption.

The ultrasonic absorption in water is attributed primarily to viscous losses. Since the classical shear (Stokes) absorption is not large enough to explain the measured absorption, the concept of a volume viscosity has been introduced. Volume and shear viscosities have similar values and seem to be related.[27] Polyelectrolyte solutions typically have a very large shear viscosity. However, this cannot be responsible for the observed ultrasonic relaxation. The absorption reported here is molecular weight independent, is not affected by excess 1–1 salts, and is increased by Ca^{2+} and Mg^{2+}. Shear viscosity, on the other hand, increases sharply with molecular weight and is decreased by the addition of excess simple salts or polyvalent counterions.

The dynamic viscoelastic behavior of polymer solutions should give rise to ultrasonic energy losses. The equations, derived by Rouse[30] and applied by Dunn[31] to ultrasonic absorption, require that $(\alpha/f^2)_r$ have an amplitude and relaxation frequency dependent both on solute molecular weight and on the shear viscosity of the solution. Hence, viscoelasticity does not seem to be the predominant observable effect in our solutions.

Dielectric dispersion in polyelectrolyte solution ($f \geq 1$ MHz) has been attributed[28] to ion atmosphere relaxation. However, the only contribution of ion atmosphere relaxation to ultrasonic absorption should be in the ΔBi term, that is, a very high-frequency contribution of small amplitude. Excess salt or alkaline earth ions should increase the ion atmosphere relaxation frequency. No such effect is observed here. Finally, the ΔBi term is the only one that depends on the overall charge density on the chain. The relaxational part of the ultrasonic absorption ($Ag(f)$ in eq 15) which is charge density independent would be due to solvent–chain segment interactions, probably through hydrogen bonding of H_2O molecules to the carboxylate groups.

It was clearly shown that the effect of different counterions was specific and that the excess absorption stopped increasing in amplitude once the number of equivalents of counterions is equal to the number of charged groups on the polyion. Figure 9 indicates at least two wide bands of relaxation times in the 1–190-MHz frequency range. However, the low-frequency band appears only with the alkaline earth counterions, while the high-frequency band is also present in Na–PA solutions.

The specific dependence of the low-frequency band on alkaline earth counterions may be considered in terms of the site-binding model depicted in Figure 1. Figure 4 shows that $(\alpha/f^2)_r/C$ for calcium acetate solutions is much smaller than that observed for Ca–CMC solutions which, in turn, is less than that for Ca–PA solutions. On the other hand, the ultrasonic behavior of calcium acetate is quite different from that of magnesium acetate, whose solutions show[32] very little excess absorption down to 2 MHz. The acetate behavior is in keeping with the view that ligand substitution rates for the alkaline earth ions are determined by the rate of solvent exchange[33] and the fact that Mg^{2+} has a very slow H_2O exchange rate compared to Ca^{2+}. The relaxation time for the Ca–PA system seems slower than for the corresponding acetate, but that of the Mg–PA solution appears substantially faster than the corresponding acetate. This suggests that both alkaline earth counterions show the same rate for the observed process but that the smaller ΔV for Mg^{2+} binding[4] accounts for the far smaller amplitude of (α/f^2) in the Mg–PA system.

For polyelectrolytes, each counterion near the chain is in an environment which does not consist of a single charged group. The idea of site binding as an interaction between isolated charged groups on the chain and single counterions is unrealistic and oversimplified, particularly for a correct description of the dynamics of the process. The flexibility of the polyionic chain makes such isolated interactions very unlikely[34] This view is supported in our results by the finding that $(\alpha/f^2)_r/C_i$, where C_i represents counterion equivalents per liter, about half as large for Ca–CMC as for Ca–PA (see Table IV), CMC being a far more rigid chain.

Table IV. $(\alpha/f^2)_r/C_i$ Comparison

Frequency	Ca^{2+}–PA^- i = 0.1	Ca^{2+}–PA^- i = 0.2	Ca^{2+}–PA^- i = 0.3	Ca^{2+}–CMC^- i = 1.0
15	1911	1654	1374	835
25	1159	893	814	522
30	934	758	674	445
50	603	455		258
130	196	152	137	122

It is also supported by the fact that $(\alpha/f^2)_r/C_i$ decreases with increasing charge density in the M^{2+}–PA^- systems since the chain is extended by electrostatic repulsion and is more rigid.

The effect found in this work will have to be taken into account when using ultrasonic absorption in an attempt to measure conformational transition kinetics for biopolyelectrolytes. It is clear that this type of counterion interaction can lead to absorption effects large in comparison to those expected from conformational changes.

The ultrasonic technique could be employed to extract more information on polyelectrolyte kinetics if it were possible to measure absorption and velocity over a wider frequency range. Such wide frequency range data could be used to construct Cole–Cole plots so as to clarify the nature of the relaxation time distributions noted in this work. It is abundantly clear that with data of more limited frequency range than reported

(30) P. E. Rouse, *J. Chem. Phys.*, 21, 1272 (1953).
(31) L. W. Kessler, W. D. O'Brien, and F. Dunn, *J. Phys. Chem.*, 74, 4096 (1970).
(32) G. Atkinson, M. Emara, and R. Fernández-Prini, manuscript in preparation.
(33) M. Eigen and G. Maas, *Z. Phys. Chem. (Frankfurt am Main)*, 49, 163 (1966); H. Diebler, M. Eigen, H. Ilgenfritz, G. Maas, and D. Winkler, *Pure Appl. Chem.*, 20, 93 (1969).
(34) Reference 13, p 244.

here, it is very difficult to identify the process responsible for the relaxation observed, not to speak of analyzing them in a quantitative manner.

Acknowledgment. The authors acknowledge the generous support of the Center of Materials Research of the University of Maryland and the Office of Saline Water, U. S. Department of the Interior. Computing time was supported by the University of Maryland Computer Science Center under National Aeronautics and Space Administration Grant No. NsG-398.

Stretched-Film Spectra and Transition Moments of Nucleic Acid Bases[1a]

Anthony F. Fucaloro[1b] and Leslie S. Forster*

Contribution from the Department of Chemistry, University of Arizona, Tucson, Arizona 85721. *Received August 3, 1970*

Abstract: The dichroic spectra of adenine, 9-methyladenine, adenosine, guanine, guanosine, cytosine, cytidine, uracil, thymine, and uridine partially oriented in stretched poly(vinyl alcohol) sheets have been recorded in the 215–300-nm region with the aim of determining the relative transition moment directions. A technique has been developed to resolve the ambiguity inherent in the stretched-film method. The 270-nm transition in guanine is perpendicular to the 250- and 220-nm transitions. In cytosine, the 270- and 235-nm transitions are nearly parallel. Evidence for a second transition in the low-energy tail of the adenine 270-nm band is presented.

Theoretical treatments of the hypochromism and circular dichroism of helical polynucleotides commonly depend upon an elucidation of the interactions among the constituent purine and pyrimidine base pairs.[2,3] A detailed knowledge of the energies, intensities, and the directions of the electronic transitions in the individual bases is requisite to any understanding of these interactions.

The spectral properties of these compounds have been extensively studied, and much is known regarding the energies and intensities of the transitions in the 180–300-nm range.[4–9] The vacuum-uv spectra have also been recorded.[10] There are still unanswered questions about possible low-intensity "hidden transitions" situated under the broad envelopes of the intense spectral bands.[4,7,8,9]

There are at least four methods that can be employed to evaluate transition moment directions: (1) polarized spectra of single crystals,[11] (2) fluorescence polarization,[9] (3) spectra of molecules embedded in stretched films,[12–14] and (4) spectra of molecules oriented in external fields.[15] The first method can give absolute transition moment directions if the crystal structure is known. However, crystal interactions may lead to erroneous results.[16] Only relative transition moment directions can be determined with methods 2, 3, and 4.

Experimental determinations of transition moment directions have been few, and in the theoretical work that requires these quantities, reliance on calculated directions has been necessary.[2,3] In view of the difficulties inherent in the experimental estimation of transition polarizations, it is likely that this situation will continue for some time. It is therefore essential that methods for the computation of transition moments be trustworthy. One goal of the present report is to ascertain the dependability of the extant calculations. A second aim of this study is to collect information about the hidden transitions present in the spectra of the purine and pyrimidine bases.

Experimental Section

Stretched-Film Dichroism. Molecules which are dissolved in a poly(vinyl alcohol) (PVA) sheet will tend to orient if the sheet is stretched. Tanizaki[12,13] has developed an expression which relates the amount of stretching of the sheet to the degree of orientation of the molecules. This assumes that the molecule possesses a unique orienting axis which tends to align along the stretch direction of the PVA sheet. In the model, an imaginary sphere formed by the randomly distributed orienting axes of the dissolved molecules is deformed into an ellipsoid of resolution of equal volume when the PVA is stretched. The stretch ratio, R_s, is the ratio of the major and minor axes of the ellipsoid. Tanizaki derived the following expression

$$2r^2 = \frac{2(T-1)+(T+1)R_d}{2T+(T-1)R_d}$$

where

$$T = R_s^2/(R_s^2-1) \times \left[1 - \left\{\frac{\pi}{2} - \tan^{-1}(R_s^2-1)^{-1/2}\right\}(R_s^2-1)^{-1/2}\right]$$

(1) (a) Based on the dissertation of A. F., submitted to the Graduate College of the University of Arizona in partial fulfillment of the requirements for the Ph.D. degree, 1969; (b) Predoctoral Fellow of the National Institute of General Medical Sciences, National Institutes of Health, 1966–1969.

(2) H. DeVoe and I. Tinoco, Jr., *J. Mol. Biol.*, 4, 518 (1962).
(3) W. C. Johnson, Jr., and I. Tinoco, Jr., *Biopolymers*, 7, 727 (1969).
(4) L. B. Clark and I. Tinoco, Jr., *J. Amer. Chem. Soc.*, 87, 11 (1965).
(5) J. W. Longworth, R. O. Rahn, and R. G. Shulman, *J. Chem. Phys.*, 45, 2930 (1966).
(6) V. Kleinwächter, J. Drobnik, and L. Augenstein, *Photochem. Photobiol.*, 6, 133 (1967).
(7) S. F. Mason, *J. Chem. Soc.*, 2071 (1954).
(8) W. Voelter, R. Records, E. Bunnenberg, and C. Djerassi, *J. Amer. Chem. Soc.*, 90, 6163 (1968).
(9) P. R. Callis, E. J. Rosa, and W. T. Simpson, *ibid.*, 86, 2292 (1964).
(10) T. Yamada and H. Fukutome, *Biopolymers*, 6, 43 (1968).
(11) R. F. Stewart and N. Davidson, *J. Chem. Phys.*, 39, 255 (1963).
(12) Y. Tanizaki, *Bull. Chem. Soc. Jap.*, 32, 75 (1959).
(13) Y. Tanizaki, *ibid.*, 38, 1798 (1965).
(14) Y. Tanizaki and S. Kubodera, *J. Mol. Spectrosc.*, 24, 1 (1967).
(15) H. Labhart, *Tetrahedron, Suppl.*, 2, 223 (1963).
(16) H. H. Chen and L. B. Clark, *J. Chem. Phys.*, 51, 1862 (1969).